

Probing the Structure and *in Silico* Stability of Cargo Loaded DNA Icosahedron using MD Simulations

Himanshu Joshi¹, Dhiraj Bhatia², Yamuna Krishnan^{3,4} and Prabal K. Maiti^{1*}

1. *Centre for Condensed Matter Theory, Department of Physics, Indian Institute of Science, Bangalore 560012, India*
2. *Institut Curie, PSL Research University, Chemical Biology of Membranes and Therapeutic Delivery unit, INSERM, U 1143, CNRS, UMR 3666, 26 rue d'Ulm, 75248 Paris Cedex 05, France*
3. *Department of Chemistry, The University of Chicago, Chicago, Illinois 60637, USA*
4. *Grossman Institute of Neuroscience, Quantitative Biology and Human Behavior, The University of Chicago, Chicago, Illinois 60637, USA*

* *To whom correspondence should be addressed. Tel: +091-80-22932865*

Fax: +91-80-23602602; Email: maiti@physics.iisc.ernet.in

Supplementary Information

1. Coordinates and dimensions of the DNA icosahedron

Each edge of the DNA icosahedron consists of a DNA helix of 26 base pairs and each vertex is made by joining five such helices with two unpaired bases at three positions at each vertex. We assume the vertex to be a circle with circumference equal to five times of the diameter of a DNA helix. The radius of this circle turns out 16 Å (by assuming the diameter of a B-DNA helix to be 20 Å)

Thus, the side length could be estimated to be 120.4 Å as follows,

$$(26 \times 3.4) \text{ \AA} + (2 \times 16) \text{ \AA} = 120.4 \text{ \AA}$$

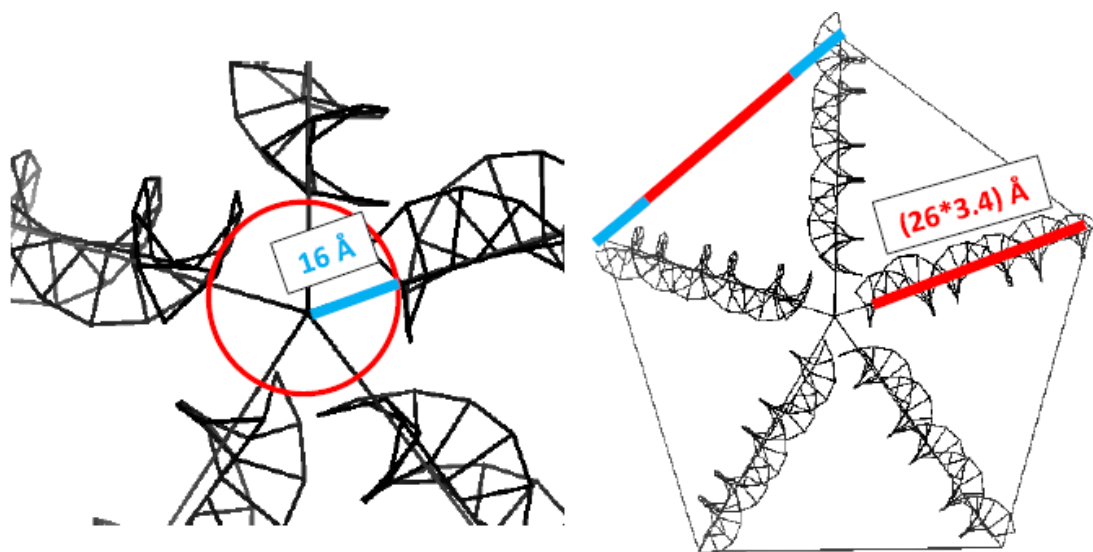
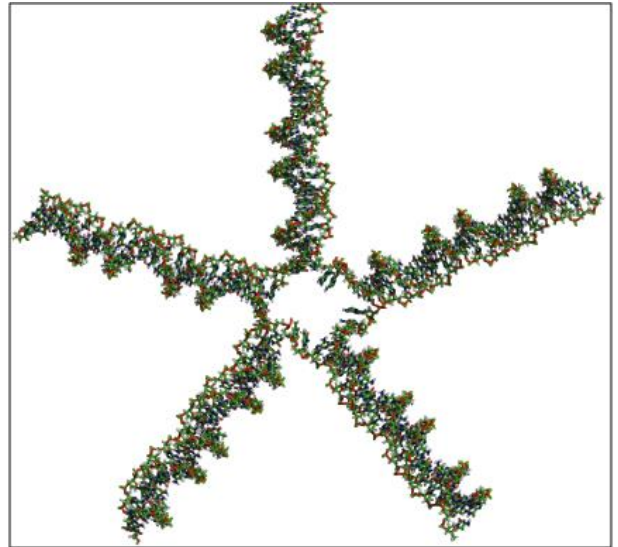
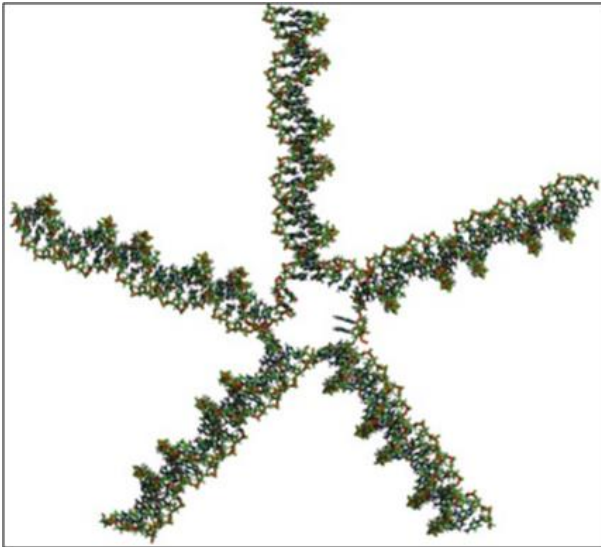


Figure S1: Schematic showing the calculation of dimensions of the edges of icosahedron:

The vertex of this 5WJ DNA polyhedral is assumed to be a circle of radius 16 Å. Thus the edge length of the ideal icosahedron has been approximated to 120.4 Å. The representative images have been drawn using ChemBioDraw.

2. The vertices and full model of icosahedral DNA.

a



b

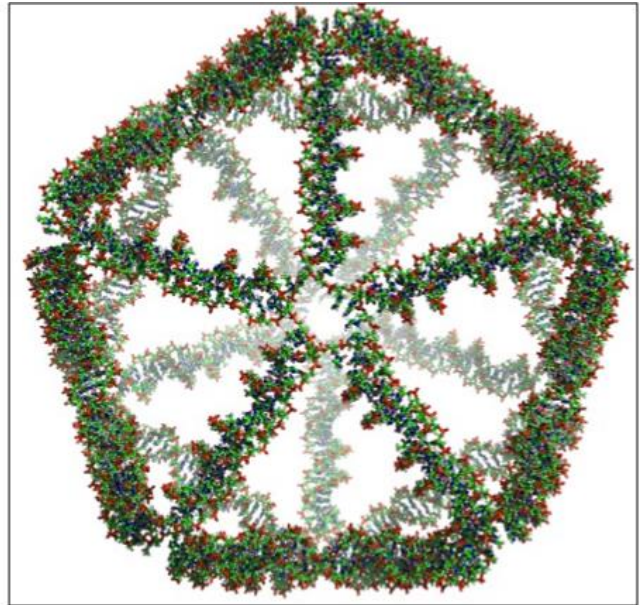
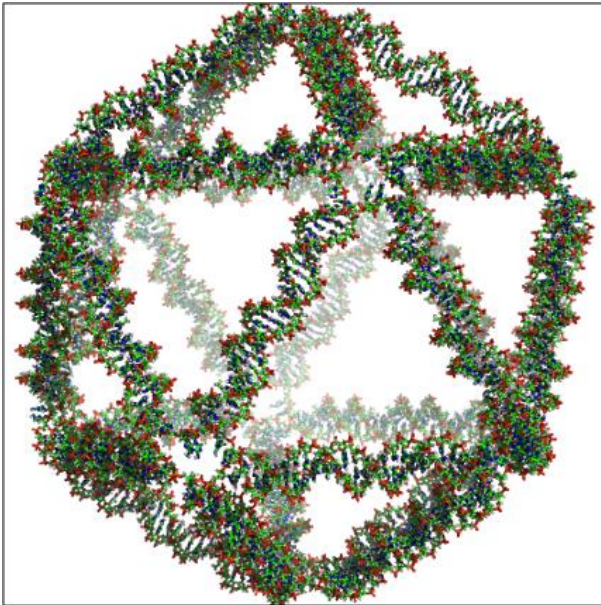


Figure S2

The atomistic model of a DNA 5WJ: (a) Top view (left) and bottom view (right) for one of the vertices. (b) Atomistic view of complete icosahedron showing C3 (left) and C5 (right) axes of symmetry.

3. The Build and Charge Neutralized Snapshots of Icosahedral DNA and AuNp Encapsulated Icosahedral DNA in Various Representations.

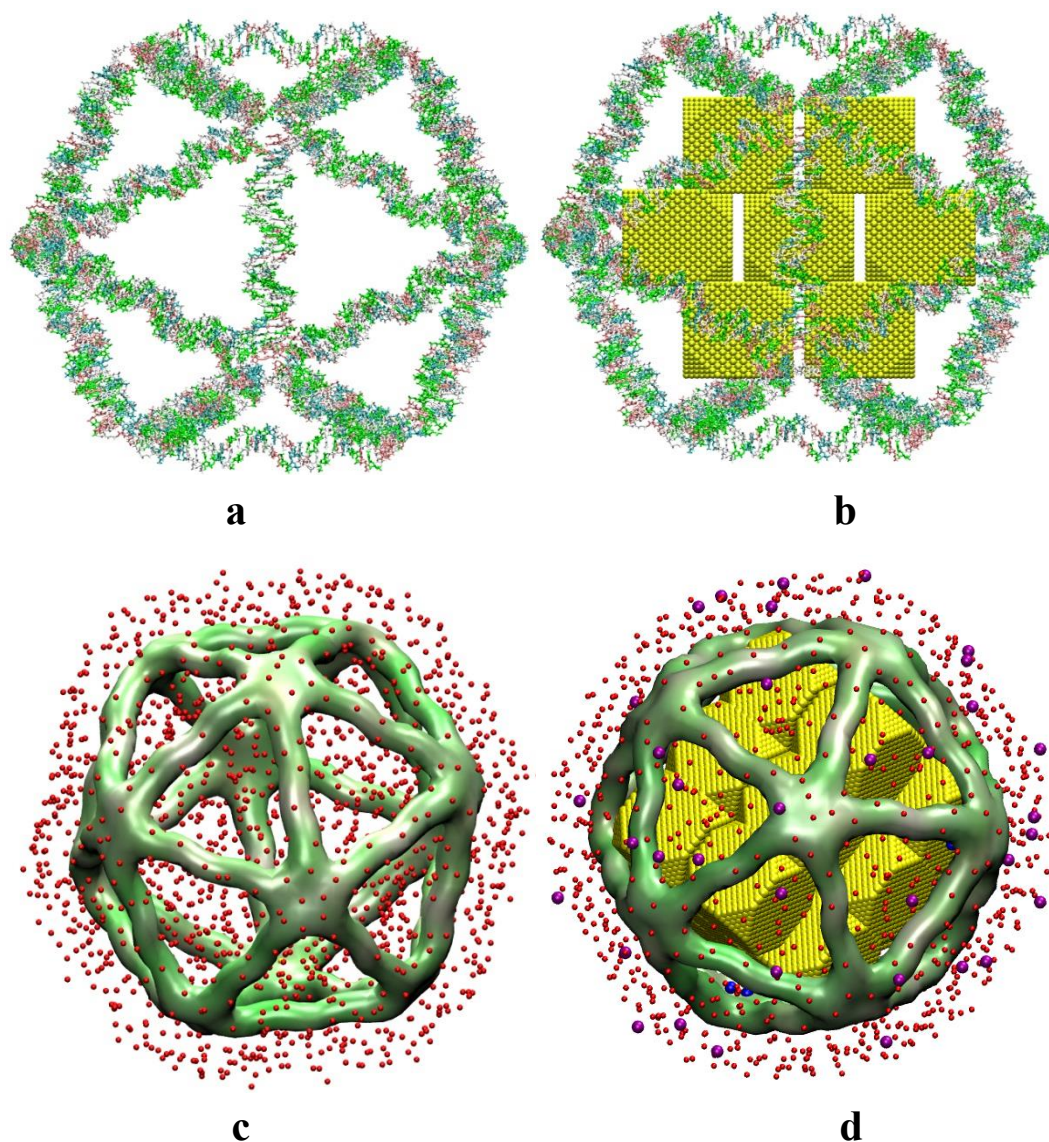


Figure S3: Snapshots of the Built Structures in Different Representations

NAB¹ built structure of (a) I_{empty} and (b) I_{AuNP} . DNA has been shown in bond representation. The placement of ions around (c) I_{empty} and (d) I_{AuNP} structure is done using the xleap module of AMBER. The ion is placed by constructing a columbic potential grid and putting the ions at electrostatically favorable positions.

4. Instantaneous Snapshots of the Simulated Structures.

The snapshots of simulation at various instant of time of atomistic simulation have been shown in the figure S4. The structure of I_{AuNP} is less distorted from its built configuration while compared I_{empty}

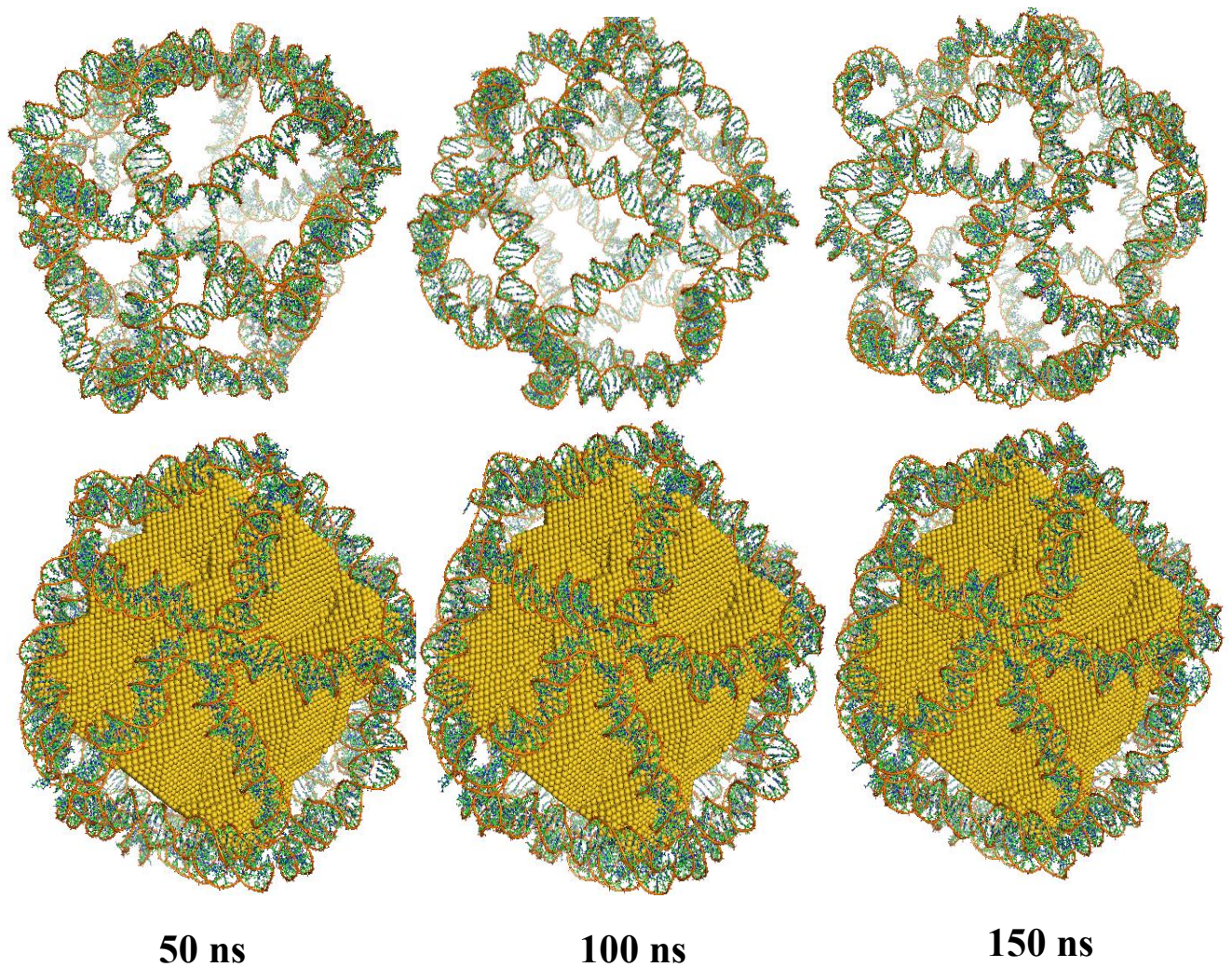


Figure S4: Structure of the DNA Icosahedron during the Simulation.

The instantaneous snapshots of I_{empty} and I_{AuNP} after 50ns, 100 ns and 150 ns MD simulation are been shown in the top and bottom panel respectively.

5. Stability of Structures: RMSF *per-Residue* and RMSF *per-Atom*

Root-Mean-Square-Fluctuation (RMSF) values have been measured for all atoms of DNA icosahedron during the MD simulation. Figure S5 (a) and S5 (b) compares per residue and per atom RMSF for the all the residues and atoms of simulated structures respectively. The RMSF values for phosphorus atoms have been highlighted in figure S5 (b) with green and blue dots. The sinusoidal nature of the RMSF reflects various edges and junctions. The RMSF values of I_{AuNP} are always lesser than I_{empty}

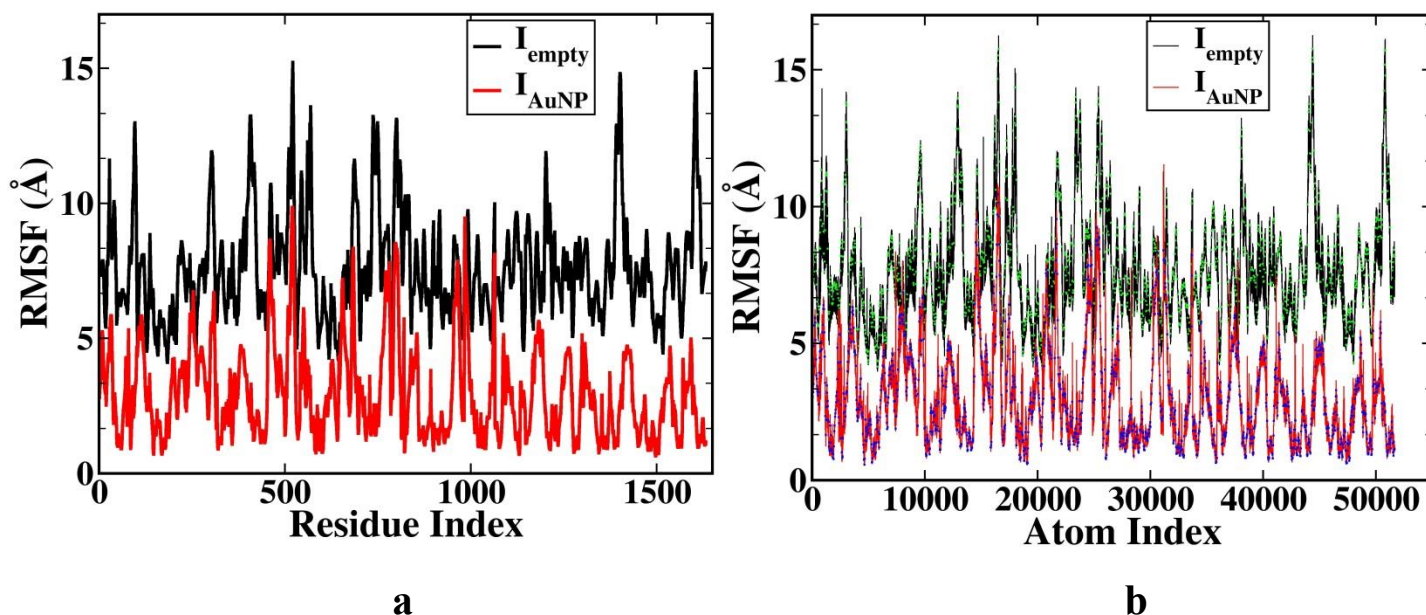


Figure S5:

(a)RMSF values per-residue (b) per atom RMSF averaged over 205 ns MD simulation for simulated structures. The RMSF values for phosphorus atoms have been highlighted in figure (b) with green and blue dots for I_{empty} and I_{AuNP} respectively. The RMSF values for I_{AuNP} is lesser than I_{empty} in both the cases.

6. Eigenvalues and Principle Component Analysis.

Principal component analysis has been performed on phosphorus atoms to identify the major modes of motion in dynamics of DNA nanostructure. It is observed from the analysis of the eigenvalues of the coordinate covariance matrix that first eigenvector accounts for the 38% and 47% of the total motion in case of I_{empty} and I_{AuNP} respectively. Since the sum of the eigenvalues is analogous of the total motion of the system, the fraction the eigenvalue to the trace (sum of eigenvalues) of matrix gives the contribution to the motion. Figure 6 (a) and (b) shows first 50 eigenvalues out of the pool of 4896 eigenvalues and their contribution to the total motion respectively.

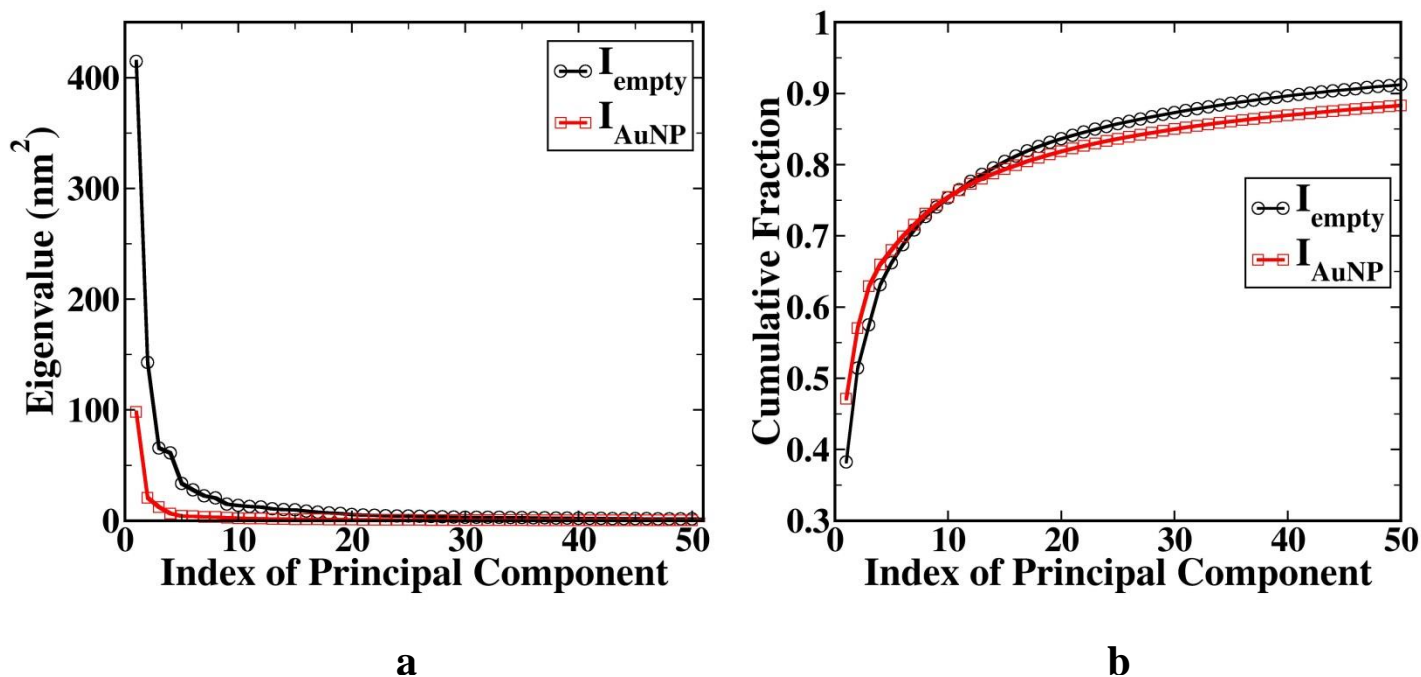


Figure S6:

(a) First 50 eigenvalues of the covariance matrix of Cartesian coordinates of phosphorus atoms during the whole simulation trajectory, (b) the cumulative contribution of corresponding eigenvectors to the motion has been shown. It is evident that first 50 eigenvectors (out of 4896) contribute for almost 90% of the total motion.

7. Time evolution of Radius of Gyration and Solvent Accessible Surface Area.

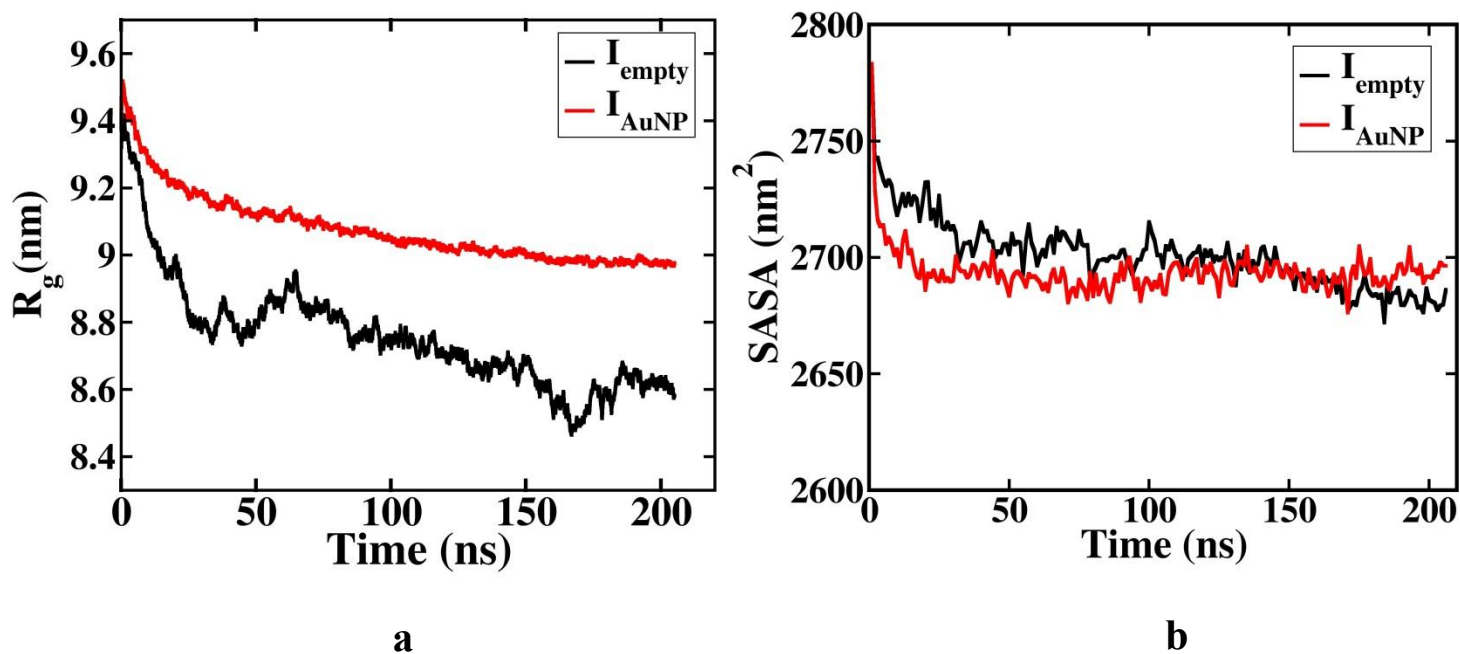


Figure S7: Time Evolution of R_g and SASA:

(a) Time evolution of the radius of gyration, R_g , of the DNA icosahedron. (b) Solvent accessible surface area, SASA, of all the atoms of icosahedral DNA using LCPO method with probe radius 1.4 Å. The analysis shows that the structures maintain icosahedral geometry during the course of simulation and also highlights the cargo bearing capability of the DNA icosahedron.

8. Conjugation of Folic Acid to DNA Icosahedron.

Folic acid (FA) has been used as a biological tag to study the endocytic pathways of cargo loaded DNA icosahedron. In order to probe the microscopic details of folate ligands to DNA icosahedron, we have come up with the atomistic model of the structure. First, we optimize the deprotonated pdb structure of FA using Gaussian09². Here, we find the wave-function of atomic orbitals via Hartree-Fock first principle calculations using 6/31G basis set to get the optimized structure (shown in figure S8 b). The partial atomic charges for the atoms of folate residue were calculated using restrained electrostatic potential (RESP) approach³. We have used the GAFF⁴ parameters to describe bonded and non-bonded interactions among FA atoms. These parameters have been generated using the antichamber module in AMBER programming suit⁵. Following the standard MD protocol, as mentioned in the simulation methodology section, we minimize and then equilibrate the FA molecule through 50 ns production run. We took the structure of the folate residue after this MD simulation to conjugate into DNA icosahedron. Prior to this conjugation, we equilibrate the structures of DNA icosahedron for 50 ns with explicit ions and water. We slightly modify the bases of DNA at some sites with amine group to attach the FA residues to icosahedron in xleap⁵. We chose the 7 sites to attach the FA residues into one particular edge of DNA icosahedron to compare the experimental results from Bhatia et al.(Bhatia et al., Nat. Nanotech. in press) The system is charge neutralized with Na⁺ ions and additionally 12 Mg²⁺ and 24 Cl⁻ ions are added for the junction stabilities. We solvate the charge neutralized DNA icosahedron into an octahedral TIP3P water box ensuring 10 Å solvent shell around solute. We perform a series of energy minimization steps to remove the bad contacts in the system. The system is gradually heated up to 300 K temperature with weak harmonic restraints (20 kcal/mol/Å²) to DNA and folate residues. Further, the system was equilibrated using NPT ensemble to attain the desired density. This is followed by 60 ns production run with no harmonic restraints to the system. We use 1 fs time step to integrate the equation of motion with 1ps⁻¹ time constant for temperature coupling with heat bath in Berendsen thermostat. We use particle mess Ewald molecular dynamics (PMEMD) approach integrated with AMBER programming environment to calculate the long range electrostatic interaction in MD simulation with periodic boundary conditions. Figure S8 (a) shows the snapshot of the structure at the end of the simulation, the folate residues has been highlighted in sphere representation while the DNA strands are shown in the surface representation. The structure of folic acid has shown in the figure S8 (b). Figure S8 (c) shows the time evolution of RMSD with respect to initially energy minimized structure. We observed the dynamics and interaction of FA molecules in conjugation to DNA icosahedron. After some deviation from initial structure, the folate conjugated DNA icosahedron (I_{FA}) takes a thermodynamically stable configuration.

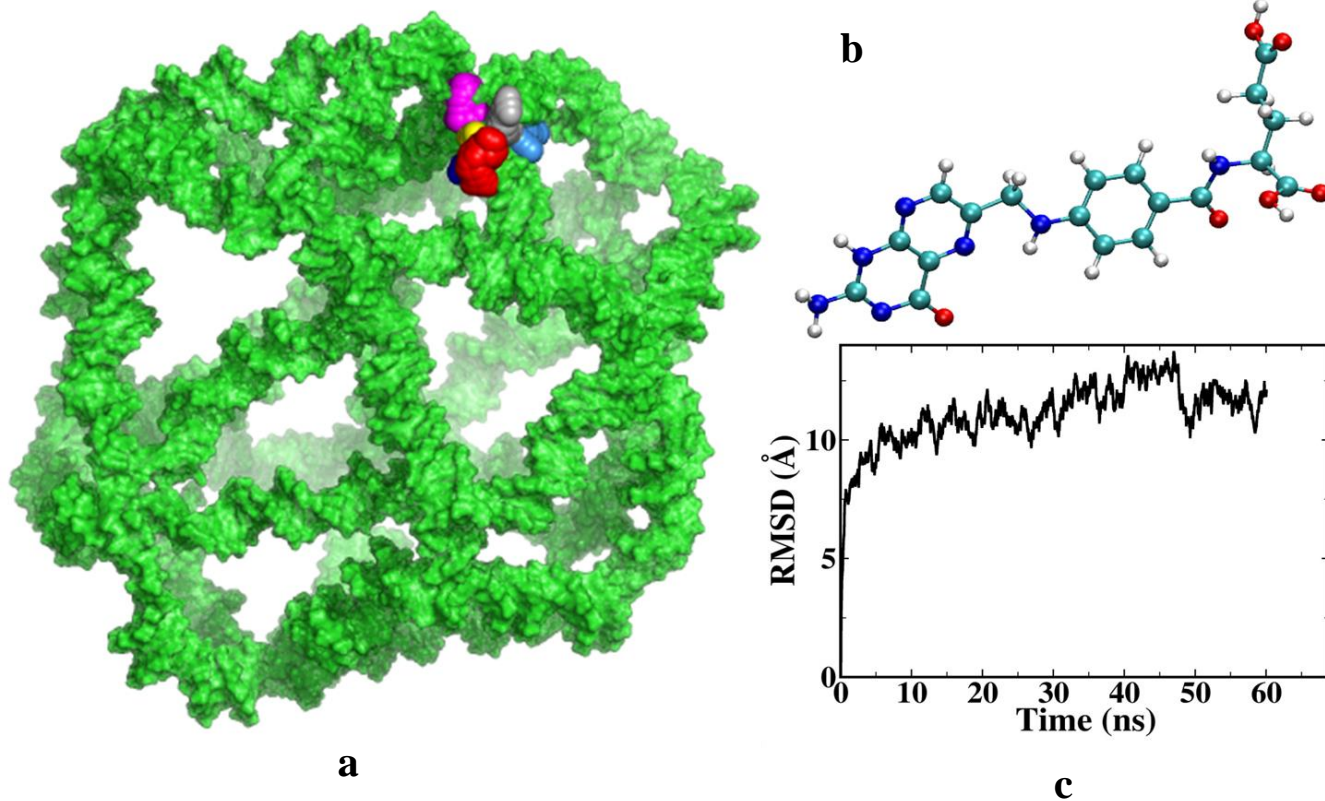


Figure S8

(a) Structure of FA conjugated DNA icosahedra after 60 ns MD simulation, the folate residues are highlighted in sphere representation and DNA strands have been shown in green surface representation. (b) Atomistic representation of folate residue. (c) The RMSD evolution of FA conjugated DNA icosahedron.

9. Conformational Analysis: Average Geometrical Parameters for the Edges of Icosahedral DNA.

We calculate various DNA helical parameters for all the duplex DNA domains comprising the edges of the DNA icosahedron in order to estimate how well the helical geometry is preserved during the simulations. The overall fluctuations in the global structural parameters of DNA (base pair, base step and helicity) during the span of the MD simulation were quantified using CPPTRAJ, analysis utility in AMBER MD programming suite.^{5, 6} Table S1a-c provided in appendix 9 of SI shows the base pair, base step and helical parameters for the duplex DNA domains in the DNA icosahedron averaged over all 30 edges respectively. The table compares the values of these three parameters at three different stages of simulations namely, prior to energy minimization, after energy minimization and after 205 ns MD simulations. The bottom row in each table shows the values of the respective parameters for 12-mer B-DNA built (B_{built}) using a standard NAB routine. Despite the relatively high standard deviation, the values of these parameters are comparable to the respective values for B_{built} . Also, all the parameters differ slightly from the structure pre-energy minimization to the structure after 205 ns MD simulation. This analysis essentially reveals that the geometry of the helix is well preserved during the simulations. A comparison of I_{empty} and I_{AuNP} revealed that the later structure shows less deformation from ideal B-DNA. We posit that the underlying extra stability of I_{AuNP} arises from host-cargo interaction that reduces thermal fluctuations of the neighboring DNA atoms. The values of twist parameter (both base-step and helical twist) reduce while compared to the built structures which is manifested to the bending of DNA helices. We observe large values of standard deviation in the above parameters but the average values are in good agreement to respective reference B-DNA parameters. The standard deviation in the parameters is largely manifested in the terminal base-pairs i.e. the base pairs at the vertices of the icosahedron. This is expected since at the vertex, the strands in a given duplex DNA domain change their helical domain/axis. The unpaired bases at the vertices (excluded for this analysis) also contribute to the deformation of ideal parameters originating from the unwinding of terminal base-pairs.⁷ The opposite ends of the edges offset the values of the parameter, so the average value is not very different with respect to the reference

structures. While, above analysis has been averaged over all the edges of the DNA icosahedron, table S2a-c in the appendix 8 of SI gives the values of these parameters for an edge A1 (chosen randomly out of 30 edges). The analysis shows that apart from the fluctuation at the vertices, the geometry of DNA is better maintained in I_{AuNP} during the course of simulation.

TableS1: Geometrical parameters of DNA averaged over all the edges.

Table S1 (a)

Base-Pair Parameters for DNA Averaged Over all the Edges of DNA Icosahedron

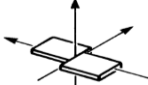
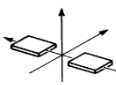
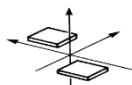
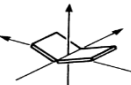
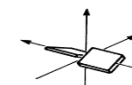
Snapshots Time	Name of the Structure	Shear (Å)	Stretch (Å)	Stagger (Å)	Buckle (°)	Propeller (°)	Opening (°)
Built	Icosahedron	0.04 (±0.45)	0.21 (±0.33)	0.36 (±0.82)	0.64 (±12.26)	-5.37 (±8.80)	4.19 (±15.91)
After energy minimization	I_{empty}	0.00 (±0.54)	0.05 (±0.36)	0.26 (±0.64)	1.20 (±16.51)	-9.96 (±11.42)	-1.74 (±12.60)
	I_{AuNP}	0.00 (±0.63)	0.06 (±0.44)	0.33 (±0.75)	0.90 (±18.63)	-11.44 (±12.32)	-0.72 (±13.54)
After 205 ns MD	I_{empty}	0.02 (±1.28)	-0.10 (±1.87)	0.03 (±1.35)	-0.31 (±19.32)	-10.25 (±15.72)	0.64 (±18.89)
	I_{AuNP}	0.01 (±1.62)	-0.08 (±1.12)	0.08 (±1.30)	0.51 (±21.50)	-9.95 (±18.90)	2.39 (±24.20)
Pictorial Representation							
Built	12-mer B-DNA	0.00 (±0.08)	0.12 (±0.03)	0.0 (±0.0)	0.0 (±0.05)	0.03 (±0.01)	0.0 (±0.08)

Table S1 (b)

Base-Step Parameters for DNA Averaged Over all the Edges of DNA Icosahedron

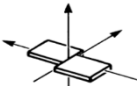
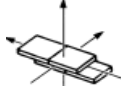
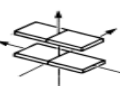
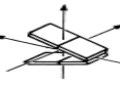
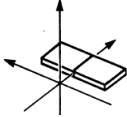
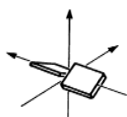
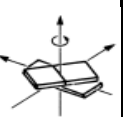
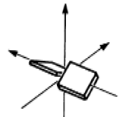
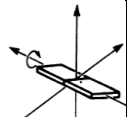
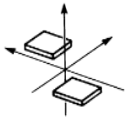
Snapshots Time	Name of the Structure	Shift (Å)	Slide (Å)	Rise (Å)	Tilt (°)	Roll (°)	Twist (°)
Built	Icosahedron	0.02 (±0.37)	-0.16 (±0.37)	3.23 (±0.32)	0.45 (±5.57)	-2.78 (±6.00)	35.86 (±4.79)
After energy minimization	I_{empty}	0.01 (±0.64)	-0.26 (±0.63)	3.25 (±0.27)	0.00 (±5.59)	-1.87 (±5.56)	35.96 (±6.34)
	I_{AuNP}	0.02 (±0.74)	-0.22 (±0.67)	3.26 (±0.37)	-0.04 (±6.51)	-1.78 (±6.73)	35.85 (±6.69)
After 205 ns MD	I_{empty}	-0.03 (±0.91)	-0.31 (±0.82)	3.37 (±0.50)	0.06 (±6.99)	3.02 (±11.18)	33.49 (±9.37)
	I_{AuNP}	0.05 (±1.27)	0.10 (±1.23)	3.42 (±0.72)	-0.49 (±9.95)	2.12 (±12.38)	34.45 (±12.41)
Pictorial Representation							
Built	12-mer B-DNA	0.00 (±0.01)	-0.27 (±0.03)	3.37 (±0.01)	0.03 (±0.27)	3.20 (±0.21)	35.71 (±1.28)

Table S1 (c)

Helical Parameters for DNA Averaged over all the Edges of DNA Icosahedron

Snapshots Time	Name of the Structure	X-disp. (Å)	Y-disp. (Å)	Helical Rise (Å)	Inclination (°)	Tip (°)	Helical Twist (°)
Built	Icosahedron	0.08 (±0.92)	0.01 (±0.94)	3.17 (±0.34)	-4.47 (±9.53)	-0.70 (±0.04)	36.82 (±4.94)
After energy minimization	I_{empty}	-0.21 (±1.16)	0.01 (±1.37)	3.20 (±0.35)	-2.80 (±9.11)	-0.29 (±0.04)	36.80 (±6.38)
	I_{AuNP}	-0.19 (±1.31)	0.00 (±1.53)	3.18 (±0.46)	-2.59 (±10.72)	-0.18 (±0.05)	37.02 (±6.74)
After 205 ns MD	I_{empty}	-1.16 (±1.95)	0.00 (±1.86)	3.22 (±0.50)	5.96 (±14.68)	-0.22 (±0.06)	34.91 (±12.68)
	I_{AuNP}	-0.47 (±2.56)	-0.12 (±2.30)	3.22 (±0.64)	4.49 (±17.56)	0.49 (±0.07)	36.73 (±15.24)
Pictorial Representation							
Built	12-mer B-DNA	0.02 (±0.03)	0.00 (±0.01)	3.38 (±0.01)	-5.21 (±0.39)	0.05 (±0.05)	35.85 (±1.27)

TableS2: Geometrical parameters for an edge of DNA icosahedron

Table S2 (a)

Average Base-Pair Parameters for an Edge of DNA Icosahedron

Snapshots Time	Name of the Structure	Shear (Å)	Stretch (Å)	Stagger (Å)	Buckle (°)	Propeller (°)	Opening (°)
Built	Icosahedron	0.00 (±0.35)	0.27 (±0.30)	0.46 (±0.77)	1.08 (±8.66)	-3.72 (±5.86)	9.94 (±15.76)
After energy minimization	I_{empty}	0.03 (±0.31)	0.09 (±0.31)	0.38 (±0.35)	0.50 (±14.88)	-7.11 (±6.79)	2.88 (±7.92)
	I_{AuNP}	-0.02 (±0.52)	0.09 (±0.35)	0.47 (±0.65)	-0.12 (±15.77)	-9.32 (±11.25)	3.67 (±9.77)
After 205 ns MD	I_{empty}	-0.03 (±0.30)	0.00 (±0.09)	0.14 (±0.38)	-1.16 (±12.14)	-9.79 (±8.62)	-0.41 (±5.38)
	I_{AuNP}	0.20 (±0.74)	0.00 (±0.14)	0.17 (±0.26)	-1.18 (±11.31)	-8.97 (±18.21)	2.70 (±9.64)
Pictorial Representation							
Built	12-mer B-DNA	0.00 (±0.08)	0.12 (±0.03)	0.0 (±0.0)	0.0 (±0.05)	0.03 (±0.01)	0.0 (±0.08)

Table S2 (b)

Average Base-Step Parameters for an Edge of DNA Icosahedron

Snapshots Time	Name of the Structure	Shift (Å)	Slide (Å)	Rise (Å)	Tilt (°)	Roll (°)	Twist (°)
Built	Icosahedron	-0.03 (±0.21)	-0.27 (±0.28)	3.30 (±0.25)	0.48 (±3.89)	-2.18 (±5.59)	35.67 (±3.00)
After energy minimization	I_{empty}	-0.05 (±0.43)	-0.38 (±0.42)	3.24 (±0.21)	0.39 (±3.57)	-0.85 (±4.32)	36.66 (±3.36)
	I_{AuNP}	-0.01 (±0.82)	-0.35 (±0.42)	3.23 (±0.24)	0.70 (±4.92)	-0.82 (±5.78)	36.93 (±4.45)
After 205 ns MD	I_{empty}	-0.02 (±1.06)	-0.14 (±0.65)	3.27 (±0.30)	0.63 (±4.08)	1.54 (±6.92)	34.46 (±4.76)
	I_{AuNP}	0.02 (±0.73)	-0.21 (±0.81)	3.31 (±0.24)	-0.92 (±4.57)	2.10 (±7.76)	35.67 (±6.34)
Pictorial Representation							
Built	12-mer B-DNA	0.00 (±0.01)	-0.27 (±0.03)	3.37 (±0.01)	0.03 (±0.27)	3.20 (±0.21)	35.71 (±1.28)

Table S2 (c)

Average Helical Parameters for an Edge of Icosahedral DNA

Snapshots Time	Name of the Structure	X-disp. (Å)	Y-disp. (Å)	Helical Rise (Å)	Inclination (°)	Tip (°)	Helical Twist (°)
Built	Icosahedron	-0.10 (±0.86)	0.12 (±0.70)	3.25 (±0.24)	-3.78 (±9.00)	-0.73 (±0.19)	36.37 (±2.86)
After energy minimization	I_{empty}	-0.49 (±0.58)	0.17 (±0.94)	3.23 (±0.25)	-1.39 (±6.62)	-0.69 (±0.16)	37.08 (±3.43)
	I_{AuNP}	-0.46 (±0.90)	0.15 (±1.54)	3.17 (±0.39)	-1.14 (±9.40)	-1.11 (±0.20)	37.72 (±4.16)
After 205 ns MD	I_{empty}	-0.46 (±1.58)	0.05 (±1.71)	3.21 (±0.45)	2.69 (±11.70)	-0.95 (±0.27)	35.41 (±4.76)
	I_{AuNP}	-0.84 (±1.81)	-0.25 (±1.24)	3.18 (±0.38)	4.49 (±12.87)	1.50 (±0.29)	36.87 (±6.31)
Pictorial Representation							
Built	12-mer B-DNA	0.02 (±0.03)	0.00 (±0.01)	3.38 (±0.01)	-5.21 (±0.39)	0.05 (±0.05)	35.85 (±1.27)

References

1. T. J. Macke and D. A. Case, in *Molecular Modeling of Nucleic Acids*, eds. N. B. Leontis and J. SantaLucia, 1998, vol. 682, pp. 379-393.
2. M. Frisch, G. Trucks, H. B. Schlegel, G. Scuseria, M. Robb, J. Cheeseman, G. Scalmani, V. Barone, B. Mennucci and G. e. Petersson, *Journal*, 2009.
3. P. Cieplak, W. D. Cornell, C. Bayly and P. A. Kollman, *J. Comput. Chem.*, 1995, **16**, 1357-1377.
4. J. Wang, R. Wolf, J. Caldwell, P. Kollman and D. Case, *J. Comput. Chem.*, 2004, **25**, 1157-1174.
5. D. A. Case, V. Babin, J.T. Berryman, R.M. Betz, Q. Cai, D.S. Cerutti, I. T.E. Cheatham, T.A. Darden, R.E. Duke, H. Gohlke, A.W. Goetz, S. Gusarov, N. Homeyer, P. Janowski, J. Kaus, I. Kolossváry, A. Kovalenko, T.S. Lee, S. LeGrand, T. Luchko, R. Luo, B. Madej, K.M. Merz, F. Paesani, D.R. Roe, A. Roitberg, C. Sagui, R. Salomon-Ferrer, G. Seabra, C.L. Simmerling, W. Smith, J. Swails, R.C. Walker, J. Wang, R.M. Wolf, X.Wu and P. A. Kollman, 2014.
6. D. R. Roe and T. E. Cheatham, III, *J. Chem. Theory Comput.*, 2013, **9**, 3084-3095.
7. M. Zgarbova, M. Otyepka, J. Sponer, F. Lankas and P. Jurecka, *J. Chem. Theory Comput.*, 2014, **10**, 3177-3189.